INSTITUTE OF PHYSICS PUBLISHING NANOTECHNOLOGY
Nanotechnology **15** (2004) S622–S627 PII: S0957-4484(04)77989-1

Overcoming the limitations of microelectronics using Si nanophotonics: solving the coupling, modulation and switching challenges

Michal Lipson

School of Electrical and Computer Engineering, Cornell University, Ithaca, NY 14853, USA

Received 8 March 2004
Published 2 August 2004
Online at stacks.iop.org/Nano/15/S622
doi:10.1088/0957-4484/15/10/020

Abstract
Optics on a silicon chip provides a new platform for the monolithic integration of optics and microelectronics and can open the door to a new technology that is free from conventional microelectronics. However, the difficulty in controlling light and diverting its path on silicon needs to be addressed before this technology can successfully be used to resolve current microelectronics bottlenecks. Here we use highly confined photonic structures for tailoring the optical mode of the structures and enhancing the electro-optical and nonlinear properties of silicon. We show high fibre to waveguide coupling efficiency and optical switching on-chip with very low powers.

1. Introduction

Si microphotonics—optics on a silicon chip—provides a new platform for the monolithic integration of optics and microelectronics. It can open the door to a new technology that is free from conventional microelectronics [1, 2] and provide low power, high bandwidth, high speed and ultra-small optoelectronic components. There are a number of fundamental challenges that need to be addressed before this technology can successfully be used to resolve current microelectronics bottlenecks. For example, the difficulty of extracting the information in and out of a chip—the equivalent to electronic soldering; and controlling light and diverting its path—the equivalent to electronic switching. This paper addresses these issues and discusses recent developments in the field.

2. Si nanophotonics—state of art

In the last few years there has been enormous progress in the field of Si nanophotonics. Currently, however, most of the proposed and demonstrated devices are either passive or are based on compound semiconductor materials and therefore remain discrete and not monolithically integrable with current CMOS (complementary metal oxide semiconductor) technology. From the system integration perspective, there is a need for active silicon devices that can be coupled to external optical fibre links.

Silicon as an optical material has unique advantages. Silicon is transparent in the range of optical telecommunications wavelengths, and is extremely mature in terms of processing. There has been a wealth of research that has mainly focused on passive integrated silicon devices. Silicon single mode waveguides with less than 0.5 μm cross-sectional dimensions have been demonstrated with low loss of the order of 0.1 dB cm^{-1} [3]. Extremely sharp curves, bends, and splitters have also been demonstrated, allowing a high level of integration [4]. Multiplexers and demultiplexers using resonant structures such as ring resonators have been shown [5, 2]. In addition, germanium detectors on silicon for 1.5 μm wavelengths have recently been demonstrated [2].

Silicon as an optical material also presents several challenges. These issues are fundamental limitations that arise from material properties, and result in the following.

(1) difficulty of externally controlling silicon structures for *optical modulation* and *switching* due to silicon's low EO and nonlinear coefficient (explained in greater detail below), and

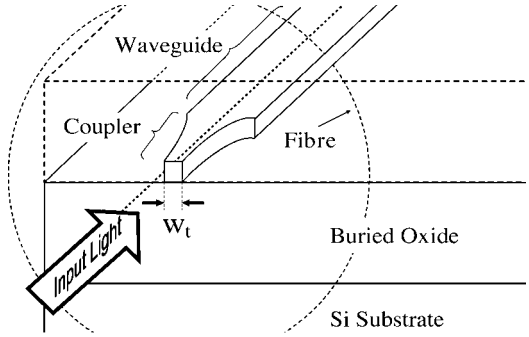

Figure 1. Schematics of a waveguide with a nano-taper coupler.

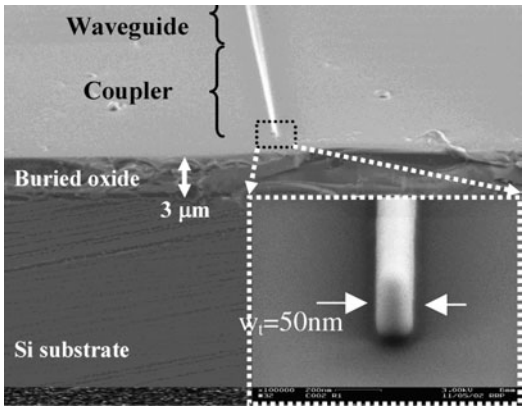

Figure 2. Scanning electron micrograph of the cleaved edge of the wafer prior to top-cladding deposition. The inset shows a zoom of a coupler tip.

(2) the necessity of *coupling* between nano-scale Si optical structures and micron-size fibres due to the current absence of an all-silicon optical source.

Coupling difficulties arise from the high index of refraction of silicon that induces high losses due to refractive index and mode mismatch between the fibres and the waveguides.

In this paper, results that overcome these limitations by using high confining structures are discussed. Light confinement can enhance the electromagnetic field in specific regions of the structures, which induces enhancement of the electro-optic and nonlinear effects in silicon. Strong light confinement also enables the engineering of the optical mode, by modifying the dimensions of the silicon waveguide.

Below, I discuss the state of the art as well as the approach for light coupling, switching and modulating on Si. In contrast to previous work, these results are based on submicron highly confined structures. It is primarily this principle, of manipulating light by confinement, that has enabled light control and coupling on silicon using ultra-compact structures.

3. Optical solder: coupling light into waveguides

Typical fibres have mode sizes of the order of $\sim$10 μm, contrasting with the submicron size of waveguides. Coupling between nano-scale waveguides and micron-size fibres has been a long-standing challenge in the field of integrated optics. This is due to both mode and index mismatch between the fibre and the waveguides, which induces coupling to radiation modes and back-reflections. To date, most of the structures suggested to alleviate this coupling problem [6–13] usually consist of a taper from the waveguide *up* to the fibre dimensions, and are either very long (millimetre size), or are difficult to fabricate. Tapers from the waveguide dimensions to the fibre dimensions, for improving coupling efficiency between optical fibre and waveguide modes, have been suggested [9]. However, in order to avoid excessive coupling to radiation modes in the taper, the required typical taper length must be of the order of millimetres. In addition, these tapers suffer from strong back-reflections at the facet of the coupler. Manolatou and Haus [7] suggest a taper based on high refractive index materials in order to decrease its length to about 5.5 μm. At the curved facet of the coupler, quarter wavelength plates are embedded, preventing back-reflections, whereas layered structures with a graded index variation are introduced in the vertical direction. Fabrication of such a structure, however, requires several steps. Inverse tapers, from the waveguide dimensions to the dimensions of a small tip, have been proposed for coupling laser diodes to optical fibres [9–11]. They rely on the evanescent field at the tip in order to increase the mode size of the waveguide to that of the fibre. These structures, however, are hundreds of microns long, and their coupling efficiencies are fundamentally limited to about 1.3 dB. This is mostly due to a high effective index mismatch between the optical fibre and the waveguide, which leads to relatively strong back-reflections.

Almeida *et al* [14] recently proposed a micrometre-long nano-taper coupler that converts *both* the mode size and the effective index of the waveguide to that of the optical fibre. The nano-taper consists of a highly confining waveguide tapered to a nanometre-sized tip at the facet, in contact with an optical fibre (figure 1). At the tip of width w_t, due to the sub-wavelength dimensions of the tip, the field profile expands, inducing a very large mode similar in effective index and profile to that of the fibre. By pointing the tip at the centre of the fibre, the light from the fibre is completely drawn into the nano-sized waveguide. Simulations based on finite difference time domain (FDTD) and beam propagation method (BPM) show that the coupling losses of the proposed device can be as low as 0.5 dB for TE-like mode at $\lambda_0 = 1550$ nm with tip width $w_t = 50$ nm. Figure 2 shows the top view of the waveguide and coupler. The inset shows the cross section of the coupler at the tip facet. The structure was fabricated using e-beam lithography and reactive ion etching (RIE). The coupling enhancement between a 5 μm MFD fibre and a single mode buried Si/SiO_2 waveguide, due to the presence of the nano-taper, was found to be eight times greater than straight coupling to the waveguide. This was measured for both TM and TE-like modes, over the 1520–1620 nm range. The authors also find that the misalignment tolerance is relatively large, with only 1 dB of additional insertion loss for $\pm$1.2 μm misalignment on both x and y directions. These results show the principle of mode conversion using ultra-compact structures. The nano-taper coupler is the shortest mode converter with high coupling efficiency on silicon. The results demonstrate the principle of mode delocalization using high confinement waveguides tapered to nanometre sizes for bridging between optical structures across size scales.

Table 1. All-silicon electro-optic modulators reported in the literature (BMFET = bipolar mode field-effect transistor; FCAM = free carrier absorption modulator; FP = Fabry–Perot; TIR = total internal reflection; ZGDC = zero gap directional coupler; M = amplitude modulation depth; J = current density; t_s = switching time; vd = vertical device; Dem.(D) = demonstrated; Prop.(P) = proposed).

Year	Author	Electrical structure	Optical structure	M (%)	J (kA cm^{-2})	Power (mW)	t_s (ns)	Length (μm)	Dem./Prop.
1987	Lorenzo *et al* [16]	p–i–n	Cross switch	50	1.26	—	—	2000	D
1989	Hemenway *et al* [17]	p–i–n	Mach–Zehnder	30	100.0	—	18	vd	D
1991	Treyz *et al* [18]	p–i–n	FCAM	75	3.0	—	50	500	D
1991	Treyz *et al* [19]	p–i–n	Mach–Zehnder	65	1.6	—	<50	500	D
1991	Xiao *et al* [20]	p–i–n	FP	10	6.0	—	25	vd	D
1994	Liu *et al* [21]	p–i–n	Y-switch	>90	9.0	—	200	800	D
1994	Liu *et al* [22]	p–i–n	TIR-switch	>90	12.5	—	100	200	D
1995	Zhao *et al* [23]	p–i–n	Mach–Zehnder	98	—	—	200	816	D
1995	Liu *et al* [24]	p–i–n	FP	80	—	—	—	20.9	P
1996	Zhao *et al* [25]	p–i–n	ZGDC	97.2	1.027	123.7	210	1103	D
1997	Cutolo *et al* [26]	p–i–n	Bragg reflector	50	—	4	24.7	3200	P
1997	Cutolo *et al* [27]	BMFET	FCAM	20	2.3	126	6	1000	P
1997	Zhao *et al* [28]	p–i–n	TIR	>88	8.8	—	110	190	D
2001	Coppola *et al* [29]	p–i–n	Bragg reflector	94	—	0.3	5	3200	P
2003	Sciuto *et al* [30]	BMFET	FCAM	75	—	160	—	400	D
2003	Barrios *et al* [31]	p–i–n	FP	80	0.116	0.025	21	20	P
2003	Barrios *et al* [32]	p–i–n	FP	80	0.61	0.014	1.3	10	P

The nano-taper coupler enables the integration of devices with different geometries on-chip. Novel devices, based on the nano-taper approach, could couple between waveguides and fibres as well as between waveguide structures with different geometries. For example, one could integrate seamlessly ridge waveguides, buried waveguides and fibres with completely different dimensions and geometries.

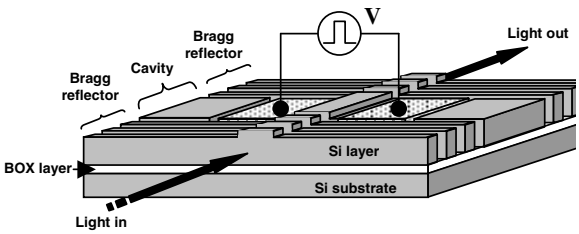

Figure 3. 1D microcavity in a silicon ridge waveguide.

4. External control of light on silicon for switching and modulating

Below I describe electro-optic and all-optical control of silicon structures for chip-scale modulators and switches. Modulators usually encode signals, while switches route signals. The difference between modulators and switches in the context of the proposed research lies in the speed, modulation depth and geometry. For switches, high modulation depth is crucial, and usually devices with at least three ports are necessary. For modulators, high speed is crucial, and devices with two ports are usually sufficient. In this section I describe the building blocks common for both switching and modulating.

5. Electro-optic devices

To date most of the work done on active devices on silicon is based on MEMS (micro-electro-mechanical systems) technology. One of the main drawbacks with MEMS is their slow response, with switching speeds of about 1–100 ms. Optical modulation can also be done using the thermo-optic effect in silicon. The thermo-optic coefficient for silicon is typically three times greater than in classical thermo-optical materials and eight times greater than in silica-based materials. The effect, however, is rather slow and can only be used for up to 1 MHz modulation frequencies [15].

An approach for faster modulation on Si is the electrical modulation of the refractive index in a specific region of planar optical devices such as Mach–Zehnder modulators, total-internal-reflection (TIR)-based structures, cross-switches, Y-switches and Fabry–Perot (FP) resonators (see table 1). The absence of mechanical elements in these devices makes them more reliable than MEMS. Table 1 shows that most of the listed devices present common features: long interaction distance and high injection current densities and power consumption in order to obtain a useful modulation depth. Most of the previously proposed Si electro-optic (EO) switches, however, are long and require high drive powers. Such length and power requirements impose difficulties in integrating these devices on-chip. There is therefore an urgent need for structures that can be implemented in a micron-size region offering low current density, low power consumption and high-modulation depth.

In [31] Barrios *et al* considers a 1D microcavity embedded in a ridge waveguide for optical switching. Highly confined optical microcavities enable the confinement and enhancement of the optical field in a very small region. The transmission of these structures is highly sensitive to small index changes in the cavity, making them adequate for intensity modulation applications in a short length [29]. In addition, since the refractive index modulation can be confined to the cavity region, the electrical power to produce the desired phase change can be made very small. Figure 3 shows a perspective schematic of the electro-optic modulator. For illustration purposes, the trenches down to the buried oxide (BOX) layer

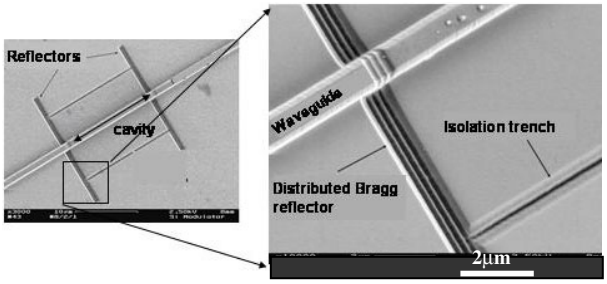

Figure 4. Scanning electron micrograph of the structure on the left.

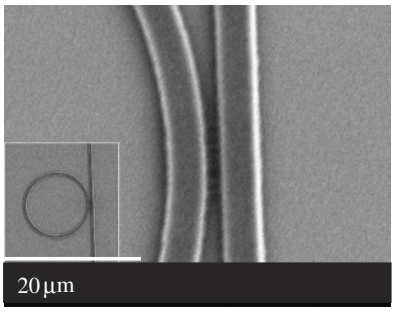

Figure 5. Scanning electron micrograph of a detail of a 10 μm diameter ring coupled to the waveguide. The inset shows the whole ring structure (the scale bar applies to the inset).

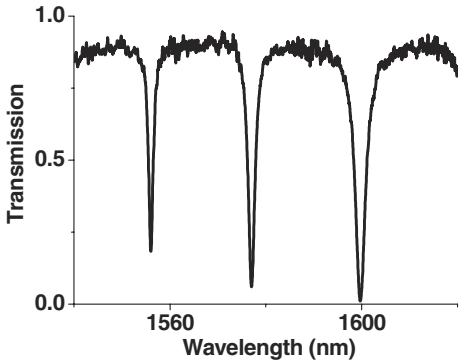

Figure 6. Measured spectrum of the 10 μm ring-resonator seen in figure 5.

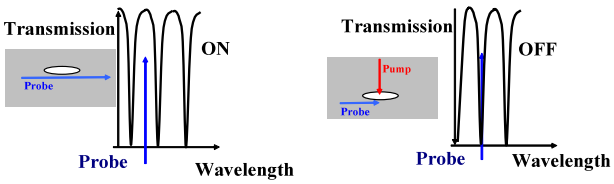

Figure 7. Typical spectra of a switch in an ON and OFF state. (This figure is in colour only in the electronic version)

are drawn as empty. In our simulations these are assumed to be completely filled with SiO_2. The device consists of an FP cavity formed by two distributed Bragg reflectors (DBRs) in a silicon on insulator (SOI) rib waveguide. Both DBRs consist of the same number of Si/SiO_2 periods down to the BOX layer. Two lateral trenches down to the BOX layer are on both sides of the rib for carrier confinement, in the region where the optical field is confined as well. Heavily doped p^+ and n^+ regions are defined in the cavity region, at both sides of the rib. Metal electrodes contact both the p^+ (anode) and n^+ (cathode) regions. Figure 4 shows a fabricated device of the passive microcavity structure (no electrical contact). Calculations show that a 20 μm long device is predicted to exhibit ~80% of modulation depth at 1.55 μm operation wavelength by using only ~25 μW of electrical power and a drive current density of 116 A cm^{-2}, leading to an increase of the device temperature $<10^{-2}$ K. The switching speed of this device is calculated to be ~16 ns, with no significant thermo-optic effect. The estimated dc power consumption for this device is at least one order of magnitude smaller than the smallest reported (theoretical) value [28]. These characteristics reveal the benefits of confining both the optical field and the injection carriers in the cavity region in order to improve the electro-optic modulator performance in terms of power consumption, current density, device length, and modulation depth. These results show the principle of strong optical and electrical confinement for electro-optical switching with ultra-low power in a micron-size Si structure.

The principle of strong confinement of light and carriers, demonstrated in these results, enables novel devices for electro-optic switches as well as modulators. The devices could include for example four port devices and devices based on embedded waveguides. Devices with different confinement levels, power dissipation and bandwidth could be tailored for different functionalities.

6. All-optical switching on a Si chip

All optical switching, i.e., controlling a probe beam with a pump beam, has been one of the holy grails in the area of photonics. It could open the door to ultra-fast circuits free of optic-to-electronic conversation, a main source of speed limitation in electro-optic devices. All-optical switching has been demonstrated in compound semiconductors [33]. In silicon, however, ultra-fast all-optical switching has been demonstrated only for vertical structures using very high pumping powers with modest signal modulations [34–36].

In [37] Almeida *et al* demonstrated all-optical modulation on a Si sub-micron-size planar structure. The modulator is based on a highly confining ring resonator. The advantage of the ring resonators is that a small change of index of refraction is sufficient for completely detuning the resonance. For a ring resonator of 10 μm, an index change as small as 10^{-3} is sufficient to tune the resonance by 1 nm. The authors study ring resonators coupled to single waveguides (see figure 5). These ring resonators transmit signals with wavelengths that do not correspond to the resonances of the ring (see figure 6). The resonances of the ring can be tuned by modifying the index of refraction of the ring (or part of the ring) and therefore a modulation of the signal transmitted through the ring resonator can be achieved (see figure 7).

Figure 5 shows a 10 μm diameter ring resonator. The inset shows the whole ring structure. The figure shows a zoom-in of part of the ring coupled to the waveguide. The devices were patterned by electron-beam lithography and subsequently etched by ICP-RIE following the same process and simultaneously with the nano-taper coupler described earlier. The spectral response of the fabricated device is shown in figure 6. One can see that the Q-value of the cavity is extremely high, demonstrating strong light confining in the

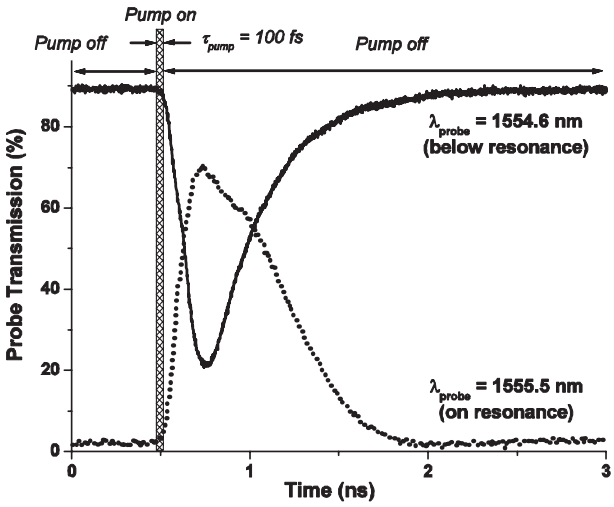

Figure 8. Temporal response of the probe signal to the pump excitation showing transmission for probe wavelengths below resonance (solid curve) and on resonance (dotted curve).

structure, which in turn signifies strong dependence on the index of refraction of the ring.

A titanium:sapphire femtosecond laser is used to generate 120 fs pulses at $\lambda_{laser} = 800$ nm with 1.5 nJ energy and 80 MHz repetition rate. The femtosecond laser pulse is converted into the pump pulse at $\lambda_{pump} = 400$ nm through second-harmonic generation using a beta-barium-borate (BBO) nonlinear crystal. The pump pulse is focused onto the single-coupled Si ring resonators. The pump pulse energy is less than 120 pJ at the ring resonator plane, which corresponds to an average optical pump power of less than 10 mW. A probe CW beam is focused into the waveguide, which is coupled to the ring resonator and collected by a 5 GHz photodetector with nominal fall/rise times of about 70 ps.

The temporal response of the transmitted probe signals are shown in figure 8 for two distinct probe wavelengths: $\lambda_{probe} = 1554.6$ nm (below resonance) and $\lambda_{probe} = 1555.5$ nm (on resonance). The measured modulation depth (MD) is defined as $MD = (I_{max} - I_{min})/I_{max}$, where I_{max} and I_{min} are, respectively, the maximum and minimum probe optical power signal for a fixed wavelength. The modulation depth is about 75% for $\lambda_{probe} = 1554.6$ nm and 97% for $\lambda_{probe} = 1555.5$ nm. The measured modulation depth is limited only by the photodetector response time. For a photodetector with a response time of less than 20 ps, one should expect to measure modulation depths of nearly 100% at both probe wavelengths.

By assuming an instantaneous spectral shift of the spectrum, followed by a simple exponential decay representing the free-carrier relaxation time, a wavelength peak shift of $\Delta\lambda = -1.1$ nm and a relaxation time of $\tau_{fc} = 450$ ps is obtained. This relaxation time, much shorter than the bulk Si free-carrier lifetime, is not fundamental, and is due to fast recombination mechanisms on the unpassivated sidewalls of the structures. By manipulating the degree of surface passivation or by using ion implantation [38], the free-carrier lifetime could be further decreased. The wavelength peak shift of the ring resonator corresponds to an effective index change of $\Delta n_{eff} = -1.45 \times 10^{-3}$, or equivalently to a refractive index change in the silicon core of $\Delta n_{Si} = -1.6 \times 10^{-3}$. This refractive index change is caused by a free-carrier concentration of $\Delta N = \Delta P = 4.8 \times 10^{17}$ cm^{-3}. Considering the physical dimensions of the ring resonator, the optical pulse energy that needs to be absorbed by the ring resonator in order to excite such a free-carrier concentration is estimated to be of only 0.9 pJ. The losses due to absorption, estimated from free-carrier concentration are $\Delta\alpha = 6.9$ cm^{-1}, significantly lower than the estimated scattering losses in the ring resonator of $\alpha_{ring} = 33.6$ cm^{-1}. The relatively low absorption losses indicate that the observed modulation is due only to a refractive index change and that thermal effects can be neglected. This is of foremost importance for the application of the proposed device as an all-optical gate, enabling near 100% transmission of the data signal once the gate is open.

These results form the basis for novel devices for all-optical Si modulators and switches, enabling entirely novel architectures on-chip. Devices confining both pump and probe with different confinement levels would enable different functionalities. One could envision for example the pump light, externally coupled to the chip, being guided in SiO_2/air waveguides for modulating Si devices in specific locations on the chip.

7. Conclusion

Recent results using sub-micron-size highly confining structures in Si show the feasibility of switching and coupling light on-chip. These results form the building blocks for all-optical circuits, where passive as well as active components could be integrated on a single chip. The devices demonstrated in this paper could form the basis for new on-chip and chip-to-chip architectures for low power and high bandwidth [39, 40] applications.

Acknowledgments

The author acknowledges support by the National Science Foundation (NSF) under contract no. ECS-0300387, by the Air Force Office of Scientific Research (AFOSR), and by the STC Program of the NSF. The author also acknowledges support by the Cornell Center for Nanoscale Systems, supported by the National Science Foundation (NSF).

References

[1] Colin Johnson R 2002 Intel reveals long-term goals for silicon photonics, sensors *EE Times* (February) (http://www.eetimes.com/semi/news/OEG20020228S0033)
[2] Kimerling L C 2000 Photons to the rescue: microelectronics becomes microphotonics *Electrochem. Soc. Interface* (Summer) **9** 28
[3] Lee K K, Lim D R, Kimerling L C, Shin J and Cerrina F 2001 Fabrication of ultralow-loss Si SiO_2 waveguides by roughness reduction *Opt. Lett.* **26** 1888
[4] Espinola R L *et al* 2001 A study of high index contrast 90 degree waveguide bend structures *Opt. Express* **8** 517
[5] Bona G-L, Denzel W E, Offrein B J, Germann R, Salemink H W M and Horst F 1998 Wavelength division multiplexed add/drop ring technology in corporate backbone networks *Opt. Eng.* **37** 3218
[6] Hauffe R, Siebel U, Petermann K, Moosburger R, Kropp J-R and Arndt F 2001 *IEEE Trans. Adv. Packag.* **4** 450

[7] Manolatou C and Haus H 2001 *Proc. LEOS Summer Topical Mtg* (New York: IEEE) p 31
[8] Alder T, Stöhr A, Heinzelmann R and Jäger D 2000 *IEEE Photon. Technol. Lett.* **8** 1016
[9] Moerman I, Van Daele P P and Demeester P M 1997 A review on fabrication technologies for the monolithic integration of tapers with III–V semiconductor devices *IEEE J. Sel. Top. Quantum Electron.* **3** 1308
[10] Kasaya K, Mitomi O, Naganuma M, Kondo Y and Noguchi Y 1993 A simple laterally tapered waveguide for low-loss coupling to single-mode fibres *IEEE Photon. Technol. Lett.* **3** 345
[11] Mitomi O, Kasaya K and Miyazawa H 1994 *IEEE J. Quantum Electron.* **8** 1787
[12] Taillaert D, Bogaerts W, Bienstman P, Krauss T F, Van Daele P, Moerman I, Verstuyft S, De Mesel K and Baets R 2002 An out-of-plane grating coupler for efficient butt-coupling between compact planar waveguides and single-mode fibers *IEEE J. Quantum Electron.* **38** 949–55
[13] Vawter G A, Sullivan C T, Wendt J R, Smith R E, Hou H Q and Klem J F 1997 *IEEE J. Sel. Top. Quantum Electron.* **6** 1361
[14] Almeida V R, Panepucci R R and Lipson M 2003 Nanotaper for compact mode conversion *Opt. Lett.* **28** 1302
[15] Cocorullo G, Iodice M and Rendina I 1994 All-silicon Fabry–Perot modulator based on the thermo-optic effect *Opt. Lett.* **19** 420
[16] Lorenzo J P and Soref R A 1987 1.3 μm electro-optic silicon switch *Appl. Phys. Lett.* **51** 6
[17] Hemenway B R, Solgaard O and Bloom D M 1989 All-silicon integrated optical modulator for 1.3 μm fibre-optic interconnects *Appl. Phys. Lett.* **55** 349
[18] Treyz G V, May P G and Halbout J-M 1991 Silicon optical modulators at 1.3 μm based on free-carrier absorption *IEEE Electron Device Lett.* **12** 276
[19] Treyz G V, May P G and Halbout J-M 1991 Silicon Mach–Zehnder waveguide interferometers based on the plasma dispersion effect *Appl. Phys. Lett.* **59** 771
[20] Xiao X, Sturm J C, Goel K K and Schwartz P V 1991 Fabry–Perot optical intensity modulator at 1.3 μm in silicon *IEEE Photon. Technol. Lett.* **3** 230
[21] Liu Y L, Liu E K, Zhang S L, Li G Z and Luo J S 1994 Silicon 1×2 digital optical switch using plasma dispersion *Electron. Lett.* **30** 130
[22] Liu Y, Liu E, Li G, Zhang S, Luo J, Zhou F, Cheng M, Li B and Ge H 1994 Novel silicon waveguide switch based on total internal reflection *Appl. Phys. Lett.* **64** 2079
[23] Zhao C Z, Li G Z, Liu E K, Gao Y and Liu X D 1995 Silicon on insulator Mach–Zehnder waveguide interferometers operating at 1.3 μm *Appl. Phys. Lett.* **67** 2448
[24] Liu M Y and Chou S 1995 High-modulation-depth and short-cavity-length silicon Fabry–Perot modulator with two grating Bragg reflectors *Appl. Phys. Lett.* **68** 170
[25] Zhao C Z, Liu E K, Li G Z, Gao Y and Guo C S 1996 Zero-gap directional coupler switch integrated into a silicon-on-insulator for 1.3 μm operation *Opt. Lett.* **21** 1664
[26] Cutolo A, Iodice M, Irace A, Spirito P and Zeni L 1997 An electrically controlled Bragg reflector integrated in a rib silicon on insulator waveguide *Appl. Phys. Lett.* **71** 199
[27] Cutolo A, Iodice M, Spirito P and Zeni L 1997 Silicon electro-optic modulator based on a three terminal device integrated in a low-loss single-mode SOI waveguide *J. Lightwave Technol.* **15** 505
[28] Zhao C Z, Chen A H, Liu E K and Li G Z 1997 Silicon-on-insulator asymmetric optical switch based on total internal reflection *IEEE Photon. Technol. Lett.* **9** 1113
[29] Coppola G, Irace A, Iodice M and Cutolo A 2001 Simulation and analysis of a high-efficiency silicon optoelectronic modulator based on a Bragg mirror *Opt. Eng.* **40** 1076
[30] Sciuto A, Libertino S, Alessandria A, Coffa S and Coppola G 2003 Design, fabrication, and testing of an integrated Si-based light modulator *J. Lightwave Technol.* **21** 228
[31] Angulo Barrios C, Almeida V and Lipson M 2003 Low-power-consumption short-length and high-modulation-depth silicon electrooptic modulator *J. Lightwave Technol.* **21** 1089
[32] Barrios C A, Almeida V R, Panepucci R R and Lipson M 2003 Electro-optic modulation of silicon-on-insulator submicron-size waveguide devices *IEEE J. Lightwave Technol.* **21** 2332
[33] Chi N, Zhang J, Holm-Nielsen P V, Xu L, Monroy I T, Peucheret C, Yvind K, Christiansen L J and Jeppesen P 2003 Experimental demonstration of cascaded transmission and all-optical label swapping of orthogonal IM/FSK labelled signal *Electron. Lett.* **39** 676
[34] Hache A and Bourgeois M 2000 Ultrafast all-optical switching in a silicon-based photonic crystal *Appl. Phys. Lett.* **77** 4089
[35] Dinu M, Quochi F and Garcia H 2003 Third-order nonlinearities in silicon at telecom wavelengths *Appl. Phys. Lett.* **82** 2954
[36] Liu Y M, Xiao X, Prucnal P R and Sturm J C 1994 All-optical switching in an asymmetric silicon Fabry–Perot etalon based on the free-carrier plasma effect *Appl. Opt.* **33** 3871
[37] Almeida V, Lipson M and Gaeta A 2004 Ultra-compact ultrafast all optical modulator, in preparation
[38] Chin A, Lee K Y, Lin B C and Horng S 1996 Picosecond photoresponse of carriers in Si ion-implanted Si *Appl. Phys. Lett.* **69** 653
[39] Mule A V, Glytsis E N, Gaylord T K and Meindl J D 2002 Electrical and optical clock distribution networks for gigascale microprocessors *IEEE Trans. Very Large Scale Integr. (VLSI) Syst.* **10** 582
[40] Miller D A B 2000 Optical interconnects to silicon *IEEE J. Sel. Top. Quantum Electron.* **6** 1312